Transactions of the Korean Nuclear Society Spring Meeting
Jeju, Korea, May 17-18, 2018

Irradiation-induced hardening and swelling of a Twinning-induced plasticity (TWIP) steel

Sangeun Kim[a], Chansun Shin[a*], Hyung-Ha Jin[b], Young-Bum Chun[b]
[a]*Department of Materials Science and Engineering, Myongji University*
[b]*Nuclear Materials Safety Research Division, Korea Atomic Energy Research Institute(KAERI)*

[*]*Corresponding author: c.shin@mju.ac.kr*

1. Introduction

Twinning-induced plasticity (TWIP) steels contain high content (15~30 wt%) of manganese, which can stabilize the austenite phase at room temperature. Deformation twinning is easily formed due to its low stacking fault energy. The formation of deformation twining induces both plastic deformation and high work hardening rate since the twinning boundaries block and accumulate dislocations. As a result, TWIP steels show both higher strength and higher elongation compared to interstitial free (IF) steels, dual-phase (DP) steels and transformation-induced plasticity (TRIP) steels.

Modification of microstructures toward forming large number of internal interfaces has been attempted in various nuclear materials with the purpose of reducing radiation damage. The tolerance to radiation damage can be enhanced by forming ample microstructural interfaces in materials. The role of these internal interfaces is to act as efficient trapping sinks and recombination sites for radiation-induced vacancies and interstitials. Vacancies and interstitials are produced in irradiated material by a cascade of atomic displacements, which are caused by the incidence of high energetic neutrons. Redistributed and recombined radiation-induced point defects and their clusters by the interfaces impede the growth of voids and the formation of large interstitial loops. Examples realizing enhanced radiation-damage resistance by increasing the density of internal interfaces are i) planar hetero-phase interfaces in multilayered nanocomposites [1], ii) increased fraction of grain boundaries in nano-grained materials [2], and iii) fine distribution of small oxide particles [3].

In this study, we investigated the irradiation hardening and swelling of a TWIP steel by using ion irradiation and He irradiation, respectively, which is rarely studied in literature. We expect that the results of this study provide valuable information on the possibility of using TWIP steels in neutron irradiation environments. Ion irradiation is often used for studying irradiation effects of a material [4-6].

2. Experimental

The composition of the TWIP steel used in this study is Fe – 9wt%Cr – 18wt%Mn – 2wt%Al. A thin plate sample was manufactured by vacuum melting and casting process followed by hot rolling.

Mechanically wet polished surface of the TWIP steel was irradiated by Fe^{3+} ions with an acceleration energy of 6.4 MeV with a dose of 2.5×10^{20} ions/m^2 using the DuET facility at the Institute of Advanced Energy, Kyoto University. The irradiation was performed in a vacuum ($2\cdot10\times10^{-5}$Pa) at a temperature of 873K. The displacement damage was calculated using the SRIM code [7]. The calculated peak damage was ~23 dpa at a depth of 1.5 μm as shown in Fig. 1.

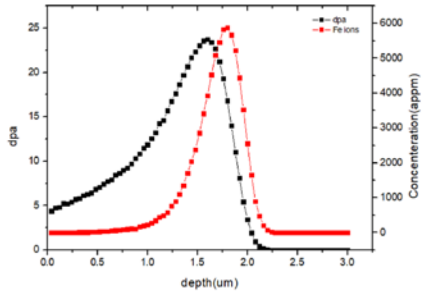

Fig. 1. The depth-DPA profile

Cross-section polishing was performed on the irradiated surface parallel to irradiation beam direction. A flat surface could be obtained on the cross-sections of the irradiated sample. EBSD analysis was performed on the irradiation-damage zone of the cross-sectional experimental samples to identify the crystal orientations of the grains. We utilized FIB milling to fabricate micro-pillars from the interior of the identified single grains. Hence, micro-compression tests could be performed on the micro-pillars with relatively constant radiation damage level. The increase in critical resolved shear stresses (CRSS) was measured from micro-compression of pillars and the Schmidt factor calculated from the measured loading direction.

A TEM grid was placed on the surface of polished specimen in order to generate He irradiated and unirradiated regions as shown in Fig. 2. The surface steps formed by swelling due to He irradiation are expected to be detected from He-irradiated holes and the screened area by the TEM grid. The specimens were He-irradiated at the KOMAC (Korea Multi-purpose Accelerator Complex) facility in Gyeongju, South Korea. The irradiation conditions are listed in Table 1.

Ion species	Energy	Fluence	Temperature
He ions	200 keV	5×10^{16}	R.T.

Table 1. The condition of ion irradiation

SRIM calculation showed 0.4 dpa-irradiation at 450 nm from the surface. After ion irradiation, these specimens are annealed 2 hours at 350 °C.

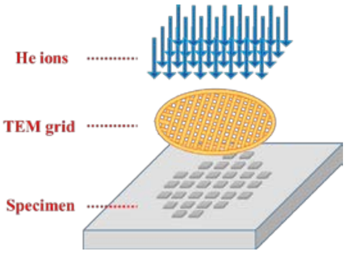

Fig. 2. Schematic design of He ion irradiation of the specimen

3. Results and discussion

Fig. 3 shows the EBSD map of the cross-section polished surface of the TWIP sample. The black circles and red circles in Figure 3(a) indicate the position of 500nm and 2μm pillars, respectively. White and black circles in Figure 3(b) indicate the location of irradiated and unirradiated pillars (D~500nm).

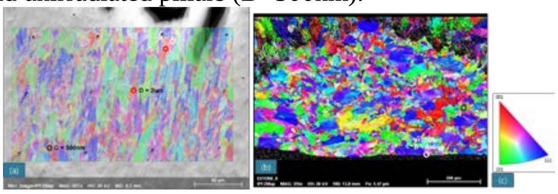

Fig. 3. EBSD maps of (a) unirradiated specimen (vibratory polished), and (b) irradiated specimen (cross-section polished)

SEM images of micropillars before and after micro-compression tests are shown in Fig. 4.

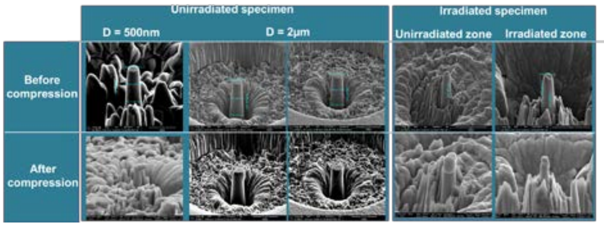

Fig. 4. SEM images of Pillars before and after micro-compression tests

Stress-strain curves and the evaluated CRSS are shown in Fig. 5. Fig. 5(a) and (b) show a small increase in stresses with decreasing micropillar size ('smaller is stronger' size effect). Figure 5(c) shows that CRSS of ion-irradiated zone is slightly increased compared to that of unirradiated zone. The loading axis measured from EBSD and the evaluated CRSS are listed in Table 2.

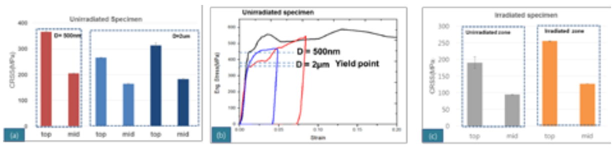

Fig. 5. (a) CRSS and (b) s-e curves of the unirradiated specimen, (c) CRSS of the irradiated specimen

		Top diameter (μm)	Mid diameter (μm)	Loading direction	Activated slip system(s)	Schmidt factor	CRSS (MPa) Top	CRSS (MPa) Mid
From unirradiated specimen	500nm pillar	0.4197	0.5591	$[21\,\bar{3}\,\bar{4}]$	$[1\,\bar{1}\,0] // (\bar{1}\,\bar{1}\,1)$	0.46	365.75	204.79
	2μm pillar	2.0228	2.57	$[33\,0\,5]$	$[1\,\bar{1}\,0] // (1\,1\,1)$ $[\bar{1}\,\bar{1}\,0] // (\bar{1}\,1\,\bar{1})$	0.46	226.73	164.53
		2.0228	2.6143	$[23\,15\,3]$	$[1\,0\,1] // (\bar{1}\,\bar{1}\,1)$	0.49	313.86	182.63
From Irradiated specimen	500nm pillar (Unirradiated zone)	0.4507	0.626	$[10\,2\,7]$	$[\bar{1}\,\bar{1}\,0] // (\bar{1}\,1\,\bar{1})$	0.48	190.55	95.18
	500nm pillar (Irradiated Zone)	0.4849	0.6863	$[7\,\bar{3}\,0]$	$[\bar{1}\,0\,1] // (\bar{1}\,1\,\bar{1})$ $[1\,0\,1] // (1\,\bar{1}\,\bar{1})$	0.49	255.91	126.76

Table 2. Loading direction, slip system, Schmidt factor and CRSS values for the compressed micro pillars.

The step-heights of the He-irradiated samples are shown in Fig. 6. The step-heights were measured by optical coherence tomography (NV-2700 the Surface Profiling System, Nanosystem cooperation)

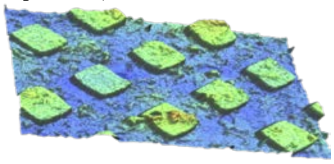

Fig. 6. Measurement the swelling effect by optical coherence tomography

4. Conclusion

We studied the effect of ion-irradiation on the yielding of a TWIP steel with the composition of Fe-18wt%Mn-9wt%Cr-2wt%Al. The CRSS evaluated by micropillar compression is ~205 MPa (evaluated using 'Mid diameter') for unirradiated TWIP specimen. This high CRSS is believed to be due to the high density of twins and dislocations generated from subsequent mechanical processes after vacuum arc melting. The specimen was ion-irradiated using 6.4 MeV Fe^{3+} ions. It is expected that the density of twins and dislocations are reduced due to exposure to high temperature (873K) during the ion-irradiation. Indeed the CRSS evaluated from the micropillars fabricated at unirradiated zone of ion-irradiated specimen (deeper than 2.5μm from the irradiated surface) is ~95 MPa (evaluated using 'Mid diameter'). The CRSS evaluated at irradiated zone of ion-irradiated specimen is ~127MPa (evaluated using 'Mid diameter'). The increase in the CRSS compared to the unirradiated zone (~95 MPa) is due to the radiation-induced dislocation loops, which are observed in TEM micrographs.

REFERENCES

[1] Gao Y, Yang T, Xue J, et al., J Nucl Mater 2011; 413: 11.
[2] Cheng GM, Xu WZ, Wang YQ, et al., Scripta Mater 2016; 123: 90.
[3] Hsiung L, Tumey S, Fluss M, et al., MRS Proceedings 2011; 1296.
[4] H. Wiedersich, J.J. Burton, J.L. Katz, J Nucl Mater, Vol.51, p. 287, 1974
[5] M. Ando, E. Wakai, et al., J Nucl Mater, 329, p. 1137–1141, 2004
[6] S. J. Zinkle, J Nucl Mater, 1, 65-98, 2012
[7] J.F. Ziegler, M.D. Ziegler, J.P. Biersack, SRIM, Nucl Instru Meth Phys Res Section B, v.268, p. 1703, 2010